Multiferroic and magnetoelectric properties of Pb0.99[Zr0.45Ti0.47(Ni1/3Sb2/3)0.08]O3–CoFe2O4 multilayer composites fabricated by tape casting

SCHILEO, Giorgio, PASCUAL-GONZALEZ, Cristina, ALGUERO, Miguel, REANEY, Ian, POSTOLACHE, P, MITOSERIU, Liliana, REICHMANN, Klaus, VENET, Michel and FETEIRA, Antonio <http://orcid.org/0000-0001-8151-7009>

Multiferroic and magnetoelectric properties of $Pb_{0.99}[Zr_{0.45}Ti_{0.47}(Ni_{1/3}Sb_{2/3})_{0.08}]O_3$–$CoFe_2O_4$ multilayer composites fabricated by tape casting

Giorgio Schileo[1], Cristina Pascual-Gonzalez[1], Miguel Alguero[2], Ian M. Reaney[3], Petronel Postolache[4], Liliana Mitoseriu[4], Klaus Reichmann[5], Michel Venet[6], and Antonio Feteira[1]

[1]*Materials and Engineering Research Institute, Sheffield Hallam University, Howard Street, Sheffield, S1 1WB, UK*

[2]*Instituto de Ciencia de Materiales de Madrid, CSIC, Cantoblanco 28049, Madrid, Spain*

[3]*University of Sheffield, Department of Materials Science and Engineering, Sir Robert Hadfield Building, Mappin Street, Sheffield, S1 3JD, UK*

[4]*A.I. Cuza University, Faculty of Physics, Blvd. Carol I 11, 700506, Iasi, Romania*

[5]*Institute for Chemistry and Technology of Materials, Graz University of Technology, Stremayrgasse 9, 8010, Graz, Austria*

[6]*Department of Physics, Federal University of São Carlos, CP-676, São Carlos, São Paulo, Brazil*

Abstract

A 2-2 type multiferroic composite device encompassing three $CoFe_2O_4$ (CFO) layers confined between four $Pb_{0.99}[Zr_{0.45}Ti_{0.47}(Ni_{1/3}Sb_{2/3})_{0.08}]O_3$ (PZT) layers was fabricated by tape casting. X-ray diffraction data showed good chemical compatibility between the two phases, whereas Scanning Electron Microscopy imaging also revealed an intimate contact between CFO and PZT layers. Under an applied electric field of 65 kV/cm, this multilayer device shows a saturated polarisation of 7.5 $\mu C/cm^2$ and a strain of 0.12%, whereas under a magnetic field of 10 kOe it exhibits a typical ferromagnetic response and a magnetic moment of 33 emu/g. These devices can be electrically poled, after which they exhibit magnetoelectric coupling.

1. Introduction

Magnetoelectric Multiferroics (MFs) exhibit simultaneously ferroelectric and magnetic order, and coupling between these two order parameters, i.e. magnetisation can be manipulated by an electric field and similarly the polarisation by a magnetic field. This phenomenon commonly referred to as the magnetoelectric (ME) effect has been envisaged as promising route to develop new electronic technologies. Unfortunately, to date no single-phase MF material was discovered, which at room temperature meets a minimum ME response required for applications. In order to overcome this limitation, many researchers have been investigating MF composites.

Basically, in MF composites the ME effect results from the product of the magnetostrictive response (i.e. a magnetic/mechanical effect) of a ferro/ferri- magnetic phase and the piezoelectric response (i.e. a mechanical/electrical effect) of a ferroelectric phase, given either as[1]:

$$ME_H effect = \frac{magnetic}{mechanical} \times \frac{mechanical}{electric}$$

or

$$ME_E effect = \frac{electric}{mechanical} \times \frac{mechanical}{magnetic}$$

The two ferroic phases can be arranged according to various geometries, as described by the phase connectivity concept introduced by Newnham et al [2]. Hence, the structure of two-phase composites can for example be referred to as 0-3, where one-phase particles (denoted as 0) are embedded in a matrix (denoted as 3). Multilayer materials, with alternated layers of dissimilar phases are referred to as 2-2 type composites, whereas the 1-3 notation is used for tubes, pillars and other elongated structures embedded into a matrix. In any of these geometries, the ME coupling will be achieved via mechanical strain, therefore a good contact between the surfaces of the two phases is essential to transfer the strain and achieve a useful ME response.

Calculations have shown that 1-3 composites of $BaTiO_3$-$CoFe_2O_4$ should display a stronger ME coupling than the corresponding 2-2 structure. However, experimental values are actually much lower than expected because of a) high porosity and/or b) high electrical conductivity due to the magnetic phase which creates conduction paths across the bulk of the material, thus preventing poling and charge storage. 2-2 multilayer structures avoid the latter issue by confining the more conductive magnetic layers between insulating ferroelectric layers. Hence, in theory, large fractions of magnetic phase can be employed as long as they are isolated between two ferroelectric layers. $CoFe_2O_4$ is often chosen as the magnetic phase because it possesses the highest magnetostrictive coefficient among oxides (~-110 to - 225 ppm), depending on sintering temperature, grain size, and other factors. The preferred ferroelectric ceramics have been $BaTiO_3$ and morphotropic $Pb(Zr,Ti)O_3$-based compositions.[3-8]

For example, Zhou et al [3] fabricated 2-2 type $PbZr_{0.52}Ti_{0.48}O_3$-$CoFe_2O_4$ composites employing a conventional uniaxial pressing technique, where the powders are alternately layered inside a mould and subsequently pressed to form the green body. Subsequently, Hao et al [9] investigated the multiferroic properties of 2-2 type $BaTiO_3$-$CoFe_2O_4$ composites fabricated by tape casting. These composites consisting of nine alternated layers of $BaTiO_3$ and $CoFe_2O_4$ exhibited a maximum ME coefficient of only 8.1 $\mu V\ cm^{-1}\ Oe^{-1}$. More recently, Yang et al [4] reported a remarkable improvement in the ME coefficient of isostatically cold-pressed $BaTiO_3$-$CoFe_2O_4$-$BaTiO_3$ laminated structures. The actual performance of those composites is dependent on the relative volumes of the two components. The best response reached 135 $mV\ cm^{-1}\ Oe^{-1}$ under a magnetic bias of 2600 Oe at 50 kHz for $0.5BaTiO_3$-$0.5CoFe_2O_4$ composites. Laminated magnetoelectric composites of $Li_{0.058}(Na_{0.535}K_{0.48})_{0.942}NbO_3$ (LKNN)/$Co_{0.6}Zn_{0.4}Fe_{1.7}Mn_{0.3}O_4$ (CZFM) prepared by the conventional solid-state sintering method were investigated by Yang et al[10], who found that compared with their particulate magnetoelectric counterparts have better piezoelectric and magnetoelectric properties due to their higher resistances and lower leakage currents. These laminated composites possess a high Curie temperature (T_C) of 463 °C, and a ME coefficient of 285 $mV\ cm^{-1}\ Oe^{-1}$. Lin et al[11] studied other Pb-free laminated composites based on laminated composites of

$(K_{0.45}Na_{0.55})_{0.98}Li_{0.02}(Nb_{0.77}Ta_{0.18}Sb_{0.05})O_3$ (LKNNTS)/$Ni_{0.37}Cu_{0.20}Zn_{0.43}Fe_{1.92}O_{3.88}$ (NCZF) and reported a ME of 133 mV cm^{-1} Oe^{-1} at a bias magnetic field of 300 Oe with the frequency of 1 kHz, which is four times as large as that of particulate composites (34 mV cm^{-1} Oe^{-1}).

Here we report the fabrication and characterisation of 2-2 type $Pb_{0.99}[(Zr_{0.45}Ti_{0.47}(Ni_{1/3}Sb_{2/3})_{0.08}]O_3$ (PZT) - $CoFe_2O_4$ (CFO) composites by tape casting instead of conventional uniaxial pressing, as this method is industrially preferred for the fabrication of integrated ceramic devices. The near the morphotropic phase boundary $Pb_{0.99}[(Zr_{0.45}Ti_{0.47}(Ni_{1/3}Sb_{2/3})_{0.08}]O_3$ composition corresponds to the commercial "soft" PZT (PIC 151) and was strategically chosen because of its extraordinary piezoelectric performance d_{33}~500 pC/N, an electromechanical coupling, k_p~0.69 and a Curie temperature of 250 °C[12].

2. Experimental

$Pb_{0.99}[(Zr_{0.45}Ti_{0.47}(Ni_{1/3}Sb_{2/3})_{0.08}]O_3$ (PZT) and $CoFe_2O_4$ (CFO) powders were prepared by the solid state reaction route. The precursor powders ($PbCO_3$, ZrO_2, TiO_2, NiO, Sb_2O_3, Co_2O_3 and Fe_2O_3 with purity ≥99% from Sigma-Aldrich, UK) were mixed and milled in high-density polyethylene (HDPE) bottles with Y_2O_3-stabilised ZrO_2 milling media and propan-2-ol as solvent for 24 h between each calcination step. $CoFe_2O_4$ was calcined at 1200°C for 8 h. The reacted powders were used to prepare the tapes, as follows: a suspension was prepared by mixing 27.6 g of ceramic powder with 5.8 g of a 1:1 mixture of ethanol and MEK (methyl ethyl ketone) and 0.346 g of Hypermer KD-1, a cationic polymeric surfactant (polyester/polyamine condensation polymer) in a HDPE bottle and ball milled overnight with Y_2O_3-stabilised zirconia milling media. Subsequently the suspension was filtered to remove the milling media, and the binder (4.62 g of a 50 % wt solution of Paraloid B-72, a thermoplastic ethylene-methyl acrylate resin, dissolved in Ethanol/MEK) and the plasticizer (1.388 g of butylbenzyl phtalate) were added to form a slurry. This slurry was mixed using a high-speed mixer (Model: Speedmixer DAC800 FVZ, Hauschild, Hamm, Germany) at 2100 rpm for 10 min and then poured behind the doctor blade in a small reservoir. The speed of the tape was set to 0.7 cm/s and the

height of the blade to 250 μm for CFO and 400 μm for PZT. The tapes were left to dry for 24 h to remove the solvent and then cut into discs of 13 mm in diameter. To fabricate the multilayers, 4 layers of piezoelectric tapes were alternatively stacked with 3 layers of magnetic materials in order to have an insulating layer on both sides of the disc. PZT-CFO laminates were pressed at 200 MPa using a Cold Isostatic Pressing (CIP). The binder and other organics were removed by heating the composites at 1 ºC/min up to 550 ºC for 5 h. After sintering, the edges were grinded off with sandpaper to avoid short-circuit due to the possible contact of ferrite layers at the edges. Purity and crystal structure were analysed using X-ray diffraction. The XRD data were collected at room temperature from powder obtained by crushing and grinding the laminates in an agate mortar, in the range 20-60 º2θ, using a high-resolution diffractometer (CuK_{α}, 1.5418 Å, D8 Empyrean XRD, PANalytical™, Almelo, The Netherlands) 45 kV and 40 mA. SEM images were collected from the cross section of multilayer laminates, coated with C and secured to the sample holder with conductive adhesive carbon pads. Room temperature Raman spectra were also collected from cross sections at 50x magnification, from 0 to 1000 cm^{-1}, using a Raman Microscope (inVia, Renishaw, UK) For dielectric and ferroelectric measurements, the opposite layers of the composites were coated with Pt paste and fired at 700ºC for 30 minutes to create electrodes. The permittivity and dielectric loss were measured between room temperature (approximately 20ºC) and 300ºC at 1ºC/min, at five different frequencies (from 1 MHz to 1 kHz) at 60 s intervals (the time it takes to measure all five frequencies is about 5 s) using a LCR meter (model e4980A, Agilent, Santa Clara, CA, USA) coupled with a furnace. Magnetic hysteresis was measured on sintered pellets under magnetic fields in the range of 0‑10 kOe with a Vibrating Sample Magnetometer (MicroMag™ VSM model 3900, Princeton Measurements, Lakeshore, Westerville, OH, USA). Ferroelectric hysteresis measurements were taken at 1 Hz using a triangular signal with the sample immersed in silicone oil using an piezoelectric evaluation system (aixPES, AixACCT, Aachen, Germany). Magnetoelectric characterization was carried out after poling the samples under an applied bias of 20 kV/cm. A system consisting of one electromagnet and one Helmholtz coil, designed to independently provide a static magnetic field up to 10 kOe (to magnetize the material), and an alternate magnetic field of 30 Oe at 25 Hz (the stimulus) was used.

Magnetoelectric output voltages (response) were monitored with a lock-in amplifier (SR830 model, Stanford Research Systems, Sunnyvale, CA, USA).

3. Results

3.1 Purity and crystal structure

The PZT sample was sintered 1140°C, whereas the PZT-CFO multilayer composites were sintered at 1050, 1100 and 1140°C for 2 h. The room temperature X-ray diffraction data for PZT and PZT-CFO multilayer composites sintered at the three different temperatures are shown Fig. 1. It can be seen that for the composite sintered at 1050°C all reflections can be assigned to either perovskite PZT or spinel CFO, whilst some unidentified parasitic phases appear when the composites are sintered at 1100°C and 1140°C, as indicated by asterisks.

Fig. 2 shows the room-temperature Raman data collected from the reference PZT sample fired 1140°C and the PZT layers confined between the CFO layers fired at 1050°C for 2h. Spectra were acquired at different points across the PZT layer, in order to monitor chemical interdiffusion between CFO and PZT and to detect any stresses resultant from potential different shrinkage rates between PZT and CFO. Hence, the position at the PZT-CFO interface is referred to as x=0, whereas the position at the middle of the PZT layer is x=0.5. In fig. 2, spectra acquired at x=0.1, 0.25 and 0.5 are illustrated. The Raman modes for PZT are labelled according the recent assignment proposed by Deluca et al [13] for the tetragonal, monoclinic and rhombohedral phases. Most of the modes associated with the tetragonal phase are labelled and the position of some indicated by vertical continuous lines. Vertical dashed lines are employed to indicate the position of some modes expected for the monoclinic phase, whilst dashed-and-dotted lines indicate the position of modes expected for the rhombohedral phase. The spectrum at x=0.5 is virtually identical to that of the reference PZT, whereas the spectrum at x=0.1, shows a slight difference concerning the relative intensities of the E + B_1 (tetragonal), $A_1(TO_2)$ (rhombohedral) and A′ modes (monoclinic). Nevertheless, in comparison with the reference PZT, neither new modes appeared nor significant Raman shifts are detected for the

spectra collected at different points from the PZT layer. Hereafter this work is focused on the device fabricated at 1050°C.

3.2 Microstructure and phase assemblage

A cross-section of the PZT-CFO composite sintered at 1050°C is shown in Fig. 3.a. This multilayer device consists of three CFO layers confined between four PZT layers and it has total thickness of ~ 735 μm. The thickness of the CFO layers (darker contrast) and inner PZT layers (lighter contrast) is of ~ 50 μm and ~100 μm, respectively, whereas the outer PZT layers are ~200 μm. There is a good contact between CFO and PZT layers, which is indicative of a successful lamination process. The grain size of CFO ranges between 1 and 2 μm, whereas PZT consists of finer grains ranging from 0.6 to 1 μm, as shown in Fig. 3.b. EDX analysis were carried out in order to access interdiffusion of elements between the CFO and PZT layers. Fig. 3.c shows results for Co and Fe EDX linescans over a PZT layer encompassed between two CFO layers. Starting in the CFO layer, the number of counts for the Fe K_α emission line approximately doubles the number of counts for the Co K_α emission line, which is consistent with the stoichiometry of $CoFe_2O_4$. The number of counts decreases continuously over a length of 10 μm at the interface between PZT and CFO, as illustrated in Fig. 3.d. for the region enclosed between by the dotted lines. Further away from the interface towards the middle of the PZT layers the number of counts is virtually negligible.

3.3 Dielectric and magnetic properties

The temperature dependence of the relative permittivity, ε_r, and dielectric loss, tan δ, for the PZT-CFO multilayers fabricated at 1050°C, is illustrated in Fig. 4. The temperature dependence of ε_r and tan δ is marked by very broad and frequency dependent maxima across differentiated temperature

ranges and thus, of different origin. At 1 kHz, ε_r increases continuously from 300 at room-temperature reaching a maximum of 3385 at 282°C, whereas at 1 MHz, ε_r increases moderately from ~45 at room-temperature to ~135 at 150°C, but then it rises rapidly to 2200 at 305°C, as shown in Fig. 4.a. This maximum signals the ferroelectric transition, and its slight shift with frequency is most probably an effect of its overlapping with dielectric relaxations rather than an indication of relaxor behaviour. At room-temperature, tan δ is 0.8 at 1 kHz, whereas at 1 MHz it drops to 0.08. This reduction of tan δ results from the shift of a loss peak towards higher temperatures with increasing frequency. Tan δ reaches a maximum of 1.6 at 150°C and 1 MHz. This peak is associated with a step in the real permittivity, and it is a common observation in magnetoelectric composites. It has been related to a Maxwell-Wagner type relaxation caused by the different conductivities of the two phases creating charge defects at interfaces [12].

The electromechanical response of a commercial PIC 151 ceramic disk with $Pb_{0.99}[(Zr_{0.45}Ti_{0.47}(Ni_{1/3}Sb_{2/3})_{0.08}]O_3)$ composition is illustrated in Fig. 5. A saturated polarisation loop showing a maximum polarisation of ~35 $\mu C/cm^2$ is observed under an electric field of 16 kV/cm. The electric coercive field, E_c, is about 10 kV/cm. The electric-field, E, induced strain, S, shows the typical symmetric butterfly-type response expected for a ferroelectric. The large hysteresis in S–E curve and the large negative strain are mainly attributed to the ferroelastic domain wall switching. For comparison the electromechanical response of the PZT-CFO multilayer device illustrated in Fig. 6. Under an applied field of 65 kV/cm it shows a maximum polarization of ~8 $\mu C/cm^2$ and an apparent electric coercive field, E_c, of ~12 kV/cm, with a tilted loop than the pure ferroelectric compound. The S-E curve is characterised by a less hysteretic behaviour and it shows lower negative strain in comparison with the commercial PIC 151 ceramic disk. The maximum bipolar strain achieved at 60 kV is about 0.12 %.

In Fig. 7, the room-temperature magnetic behaviour of the PZT-CFO multilayer device and CFO is compared. The shape of the magnetic loop for the CFO-PZT matches the shape of the hysteresis loop for CFO. Moreover, taking into account that the saturated magnetisation, M_s, for CFO is around 82

emu/g, the lower value of 33 emu/g for the PZT-CFO multilayer is in good agreement with the weight fraction of CFO in the device. Also the ratio between the remanent magnetisation of CFO and PZT-CFO is similar to the ratio between their maximum magnetisations. The coercivity for the device is ~ 500 Oe, which is slightly higher than the coercivity of pure CFO and to reach nearly fully magnetisation it is required to apply at least 3.5 kOe.

Finally, Fig. 8 shows that magnetoelectric coupling is established between the CFO and PZT layers in this device. A typical magnetoelectric curve is found with a maximum transverse magnetoelectric coefficient α_{31} of ≈11.6 mV cm^{-1} Oe^{-1} under a bias magnetic field of ≈1.65 kOe. Piezoelectric thickness has been used for normalization.

4. Discussion

The performance of conventional strain-mediated multiferroic composites is strongly dependent on the microstructure and the coupling interaction across the ferroelectric - ferromagnetic interfaces. The interface coupling is reliant on surface homogeneity, thereby any parasitic interfacial phases formed during the high temperature fabrication process will reduce the displacement transfer capability of the magnetostrictive and piezoelectric phases. In the present study, it is demonstrated that the fabrication of the CFO-PZT multilayer device needs to be carried out at temperatures no higher than 1050°C, otherwise considerable amounts of parasitic phases will form at the interface between CFO and PZT, as shown by the X-ray diffraction data in Fig. 1. In addition, EDX analyses also showed that PZT layers in the proximity of the interface with CFO are enriched with Fe and Co, as shown in Fig. 3.d. This clearly suggests an unavoidable interdiffusion at the interface during the sintering process. Previously, Zhou et al [3] found ion interdiffusion between CFO and $PbZr_{0.52}Ti_{0.48}O_3$ layers during high-temperature sintering process to reduce the saturation magnetostriction of CFO and also to alter the properties of the PZT layers. Indeed, they observed that diffusion of Pb, Ti and Zr into the CFO reduces the saturation magnetostriction from −200 ppm down to -150 ppm and reduces the magnetic field for saturation. Moreover, they also observed a small reduction in the coercivity of CFO in the composites. In contrast, in the present study coercivity increases from 400 ~Oe for the bulk CFO to ~500 Oe for the CFO-PZT multilayer device, as illustrated in Fig. 7. Several reasons may account for

this difference, such as: a) the different sintering temperature influences the particle size and this in turn has an impact on the coercivity, and/or b) a small amount of Ti, Zr and other elements has entered the CFO lattice, influencing the domain mobility. To support this hypothesis, it is useful to compare the results of Chae et al [14], whose study shows a 20% Ti doped $CoFe_2O_4$ sintered at 1050ºC with a coercive field of approximately 500 Oe.

Now considering in more detail the impact of element interdiffusion into the PZT layers it is convenient to recall the synchrotron data analysis carried out by Kounga et al [12] on commercial $Pb_{0.99}[Zr_{0.45}Ti_{0.47}(Ni_{1/3}Sb_{2/3})_{0.08}]O_3$. According to those investigators, in this near MPB composition the tetragonal and monoclinic symmetries coexist in a 3:1 ratio. Nevertheless, these authors also mentioned that some nanodomain regions that are interpreted as monoclinic may not have strictly this internal structure. Indeed the Raman data in Fig. 2, can be mainly associated to tetragonal symmetry, but both monoclinic and rhombohedral symmetries may also coexist. In regions near the CFO interface, the $A_1(TO_2)$ mode for the rhombohedral symmetry appears to increase in intensity. Actually, there is a remarkable similarly between this and the spectrum reported by Souza Filho et al [15] for $Pb(Zr_{1-x}Ti_x)O_3$ with x=0.47, which was described to have intermediate properties from those of x=0.46 (rhombohedral) and x=0.48 (tetragonal). The changes in line shape in 490-640 cm^{-1} region might be due to the coexistence of monoclinic and tetragonal phases, as reported by Noheda et al [16]. For tetragonal symmetry, $A_1(TO)$ modes are associated with the ferroelectric nature of PZT. Hence, the $A_1(TO_1)$ soft mode originates from displacements of the Pb ions in relation to the Ti/Zr and O ions, whereas the $A_1(TO_2)$ mode consists of displacements of Ti/Zr ions with respect to both oxygen and Pb ions. Finally, the $A_1(TO_3)$ originates from displacements of Ti/Zr ions in the c-axis direction together with the O ions. CFO and PZT also have commensurate lattice parameters ($a_{CFO}=2a_{PZT}$), therefore one would expect negligent lattice mismatch at the interface between those two phases. This is partially corroborated by the absence of Raman shift even for regions near the interfaces.

The confinement of CFO between 2 layers of PZT circumvents conductivity issues, commonly observed in 1-3 type multiferroic composites [17]. Due to the high electrical conductivity of CFO the electric field percolates throughout the alternated layers of PZT and CFO enabling domain switching

of the PZT phase, as shown by the bipolar measurements of the polarisation and strain in Fig. 6. However, it is worth to note that for a given external voltage, each PZT layer is subjected to a reduced voltage by comparison as in the bulk PZT ceramics (four times, if one accepts that CFO does not polarize at all) and therefore, the needed field for the full saturation of the device is higher than for the pure ferroelectric compound, as observed. The layered composite has an overall lower polarisation with a tilted character of its P(E) loop and consequently, it also shows a smaller piezoelectric coefficient and piezoelectric strain. Hence, both the lower polarisation and piezoelectric response in the layered structure are the result of both a lower voltage applied to an individual ferroelectric layer as well as to the small compositional modifications (doping of PZT with Fe and Co) at the ferrite-ferroelectric interfaces which makes the ferroelectric layer less homogeneous from the switching and piezoelectric point of view. Even small doping of PZT with Fe and Co causes the development of acceptor-oxygen vacancy defect dipoles that enhance the coercive and saturation field and tend to reduce the domain wall motion at interfaces, thus resulting in lowering the total polarisation, with respect with pure PZT material. The aforementioned may be at the origin of the smaller negative strains observed in the composites in relation to commercial PIC 151, however this still deserves further investigations.

On the other hand, the difference in conductivity between the magnetic and dielectric oxides and the acceptor-oxygen vacancy defects located at the interfaces are responsible of the Maxwell-Wagner type dielectric relaxation found between RT and the ferroelectric transition temperature [12]. Finally, magnetoelectric measurements, Fig. 8, show coupling to be established between the ferroelectric and ferrimagnetic layers; the value of the magnetoelectric (ME) coefficient α_{31} ≈11.6 mV cm^{-1} Oe^{-1}) is slightly lower than those of three-layer $PbZr_{0.52}Ti_{.48}O_3$-$CoFe_2O_4$-$PbZr_{0.52}Ti_{.48}O_3$ composites fabricated uniaxial pressing [3]. Indeed, α_{31} coefficients of ~15 and 50 mV $cm^{-1}Oe^{-1}$ were reported for magnetic volumetric fractions of 0.15 and 0.28, respectively, to be compared with a fraction of 0.22 in the current case. Coefficients are expected to increase with the magnetic volumetric fraction, and a value of ~150 mV $cm^{-1}Oe^{-1}$ was achieved in [3] for a fraction of 0.71. Any imperfection at the interface will decrease the displacement transfer capability, leading to a decrease in the ME response in 2-2 type

multilayer devices. Future work is required to both theoretically calculate the maximum ME achievable for this particular two component system and measure the response at variable fields and frequencies, and with larger magnetic volumetric fraction.

Conventional microelectronics circuitry requires integrated devices. This motivated the present investigation on the processability of a 2-2 type multiferroic PZT-CFO multilayer device by tape casting, which is the preferred industrial process for the fabrication of multilayered ceramic devices. In this work it is demonstrated that PZT-CFO laminates can be successfully fabricated, while retaining the properties of the parent components. Moreover, coupling between those components was also demonstrated.

5. Conclusion

A 2-2 type multiferroic PZT-CFO multilayer device encompassing three $CoFe_2O_4$ (CFO) layers confined between four $Pb_{0.99}[Zr_{0.45}Ti_{0.47}(Ni_{1/3}Sb_{2/3})_{0.08}]O_3$ (PZT) layers was successfully fabricated by tape casting. Trough adjustment of the sintering temperature it was possible to limit the interdiffusion of elements between the PZT and CFO layers preventing the formation of secondary phases, and thereby retaining the ferroelectric and ferromagnetic characteristics. Moreover, the coexistence of ferroelectricity and ferromagnetism in this device combined with an intimated contact between the layers enables a significant ME response.

Acknowledgments

The authors would like to thank the financial support of the Cristian Doppler Research Association and of TDK EPC, a company from the TDK Corporation. MA thanks funding by Spanish MINECO through project MAT2014-58816-R. AF acknowledges SHU's Strategic Research Infrastructure Fund for the acquisition of the AixACCT system.

References

[1] C.-W. Nan, M.I. Bichurin, S. Dong, D. Viehland, G. Srinivasan, Multiferroic magnetoelectric composites: Historical perspective, status, and future directions, Journal of Applied Physics 103(3) (2008) art. nº 031101.

[2] R.E. Newnham, D.P. Skinner, L.E. Cross, Connectivity and piezoelectric-pyroelectric composites, Materials Research Bulletin 13(5) (1978) 525-536.
[3] J.P. Zhou, H.C. He, Z. Shi, G. Liu, C.W. Nan, Dielectric, magnetic, and magnetoelectric properties of laminated $PbZr_{0.52}Ti_{0.48}O3/CoFe_2O_4$ composite ceramics, Journal of Applied Physics 100(9) (2006) art. nº 094106.
[4] H.B. Yang, G. Zhang, Y. Lin, Enhanced magnetoelectric properties of the laminated $BaTiO_3/CoFe_2O_4$ composites, Journal of Alloys and Compounds 644 (2015) 390-397.
[5] T. Walther, N. Quandt, R. Koferstein, R. Roth, M. Steimecke, S.G. Ebbinghaus, $BaTiO_3$-$CoFe_2O_4$-$BaTiO_3$ trilayer composite thin films prepared by chemical solution deposition, Journal of the European Ceramic Society 36(3) (2016) 559-565.
[6] C. Schmitz-Antoniak, D. Schmitz, P. Borisov, F. de Groot, S. Stienen, A. Warland, B. Krumme, R. Feyerherm, E. Dudzik, W. Kleemann, H. Wende, Electric in-plane polarization in multiferroic $CoFe_2O_4/BaTiO_3$ nanocomposite tuned by magnetic fields, Nature Communications 4 (2013) art. nº 2051.
[7] V. Corral-Flores, D. Bueno-Baques, R.F. Ziolo, Synthesis and characterization of novel $CoFe_2O_4$-$BaTiO_3$ multiferroic core-shell-type nanostructures, Acta Materialia 58(3) (2010) 764-769.
[8] L.P. Curecheriu, M.T. Buscaglia, V. Buscaglia, L. Mitoseriu, P. Postolache, A. Ianculescu, P. Nanni, Functional properties of $BaTiO_3$-$Ni_{0.5}Zn_{0.5}Fe_2O_4$ magnetoelectric ceramics prepared from powders with core-shell structure, Journal of Applied Physics 107(10) (2010) art. nº 104106.
[9] L.B. Hao, D.X. Zhou, Q.Y. Fu, Y.X. Hu, Multiferroic properties of multilayered $BaTiO_3$-$CoFe_2O_4$ composites via tape casting method, Journal of Materials Science 48(1) (2013) 178-185.
[10] H.B. Yang, J.T. Zhang, Y. Lin, T. Wang, High Curie temperature and enhanced magnetoelectric properties of the laminated $Li_{0.058}(Na_{0.535}K_{0.48})_{0.942}NbO_3/Co_{0.6}\ Zn_{0.4}Fe_{1.7}Mn_{0.3}O_4$ composites, Scientific Reports 7 (2017) art. nº 44855.
[11] Y. Lin, J.T. Zhang, H.B. Yang, T. Wang, Excellent piezoelectric and magnetoelectric properties of the $(K_{0.45}Na_{0.55})_{0.98}Li_{-0.02}(Nb_{0.77}Ta_{0.18}Sb_{0.05})O_3/Ni_{0.37}Cu_{0.20}Zn_{0.43}Fe_{1.92}O_{3.88}$ laminated composites, Journal of Alloys and Compounds 692 (2017) 86-94.
[12] A.B. Kounga, T. Granzow, E. Aulbach, M. Hinterstein, J. Rodel, High-temperature poling of ferroelectrics, Journal of Applied Physics 104(2) (2008) art. nº 024116.
[13] M. Deluca, H. Fukumura, N. Tonari, C. Capiani, N. Hasuike, K. Kisoda, C. Galassi, H. Harima, Raman spectroscopic study of phase transitions in undoped morphotropic $PbZr_{1-x}Ti_xO_3$, Journal of Raman Spectroscopy 42(3) (2011) 488-495.
[14] K.P. Chae, W.K. Kim, J.G. Lee, Y.B. Lee, Magnetic properties of Ti-doped ultrafine $CoFe_2O_4$ powder grown by the sol gel method, Hyperfine Interactions 136(1-2) (2001) 65-72.
[15] A.G. Souza, K.C.V. Lima, A.P. Ayala, I. Guedes, P.T.C. Freire, F.E.A. Melo, J. Mendes, E.B. Araujo, J.A. Eiras, Raman scattering study of the $PbZr_{1-x}Ti_xO_3$ system: Rhombohedral-monoclinic-tetragonal phase transitions, Physical Review B 66(13) (2002) art. nº 132107.
[16] B. Noheda, D.E. Cox, G. Shirane, J.A. Gonzalo, L.E. Cross, S.E. Park, A monoclinic ferroelectric phase in the $Pb(Zr_{1-x}Ti_x)O_3$ solid solution, Applied Physics Letters 74(14) (1999) 2059-2061.
[17] G. Schileo, A. Feteira, I.M. Reaney, P. Postolache, L. Mitoseriu, K. Reichmann, Characterization of Yttrium Iron Garnet/Barium Titanate Multiferroic Composites Prepared by Sol-Gel and Coprecipitation Methods, International Journal of Applied Ceramic Technology 11(3) (2014) 457-467.

List of Figures

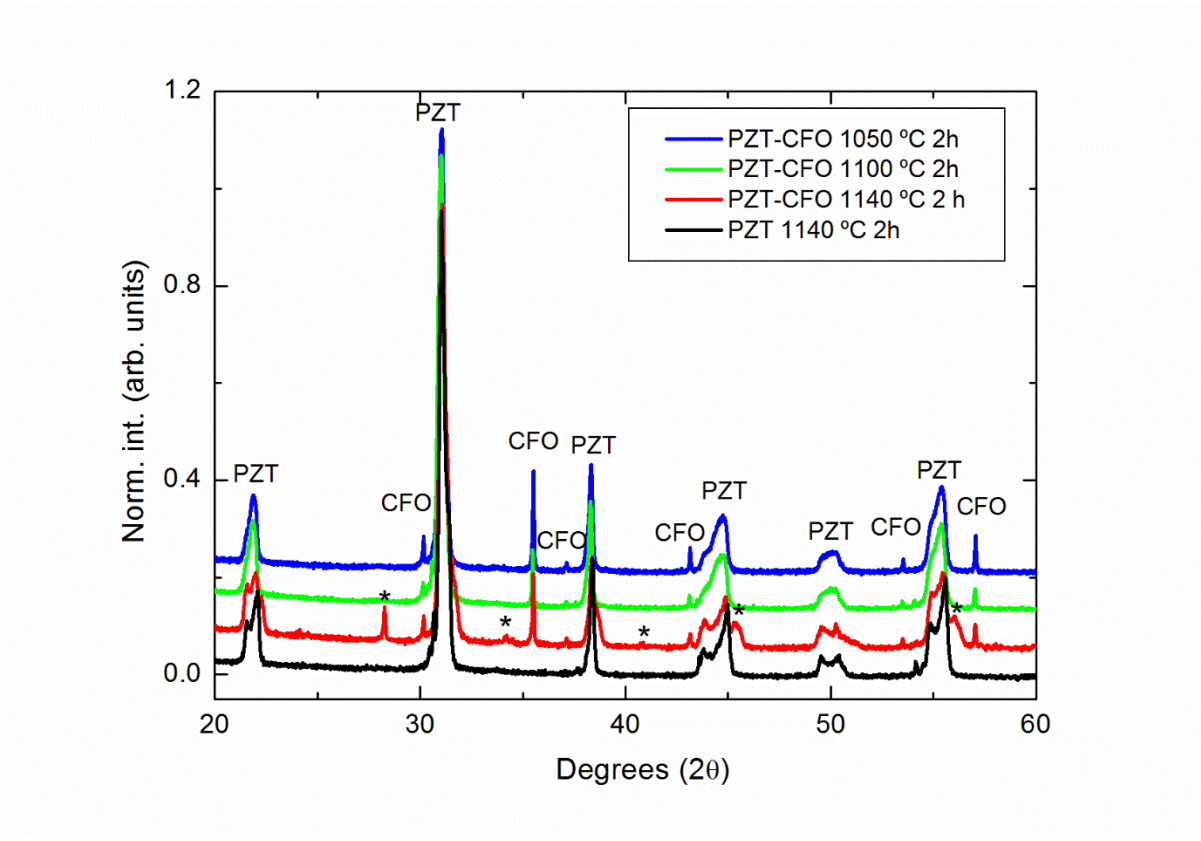

Fig. 1 Room-temperature X-ray diffraction data for PZT ceramics sintered 1140°C and PZT-CFO multilayer composites were sintered at 1050, 1100 and 1140°C for 2 h.

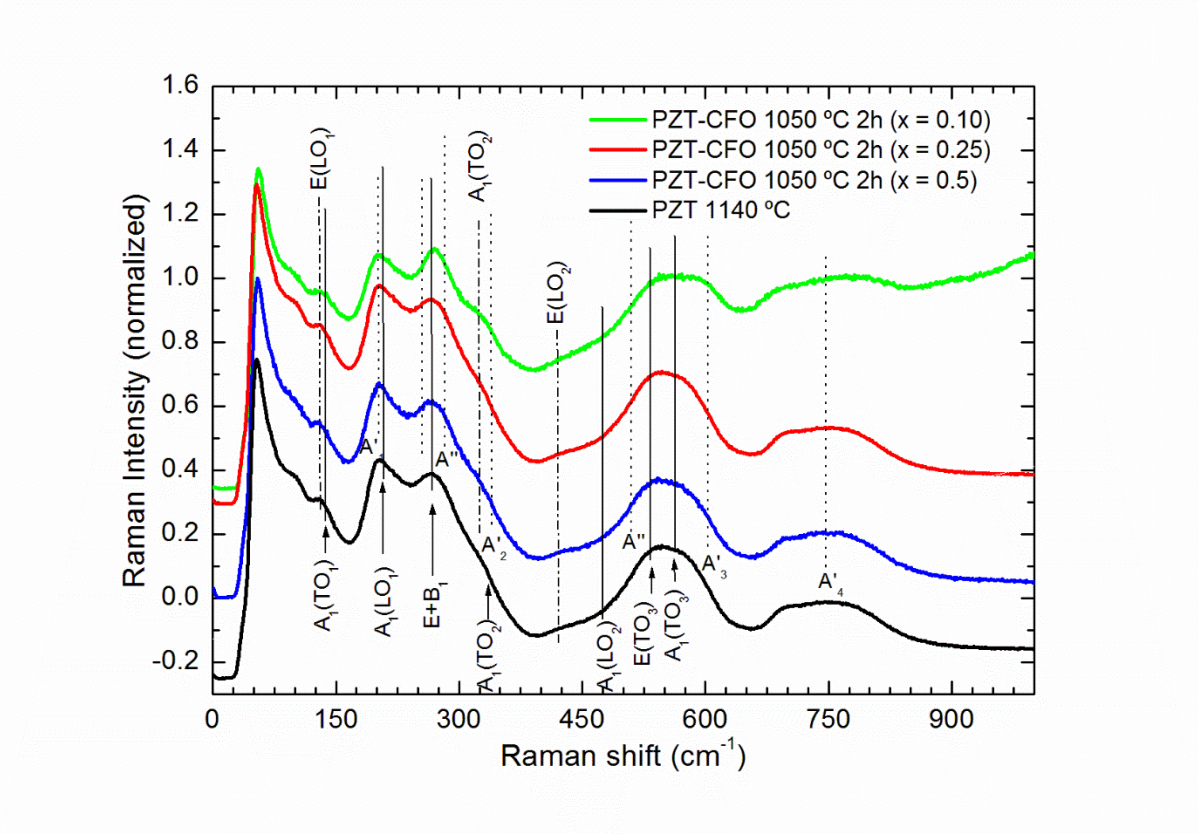

Fig. 2 Room-temperature Raman spectra acquired across the PZT layer.

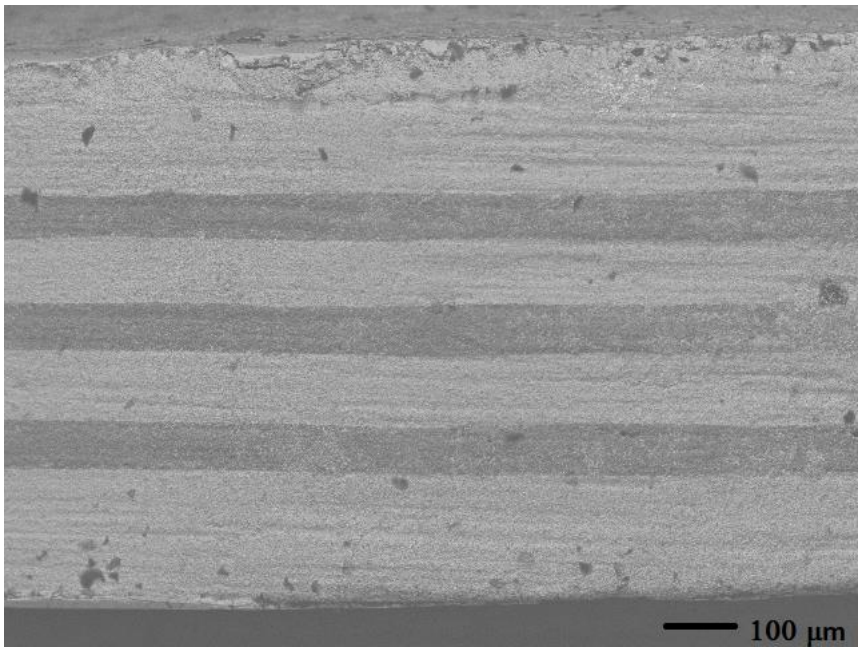

Fig. 3.a SEM micrograph of the cross-section for the PZT-CFO composite sintered at 1050°C for 2h.

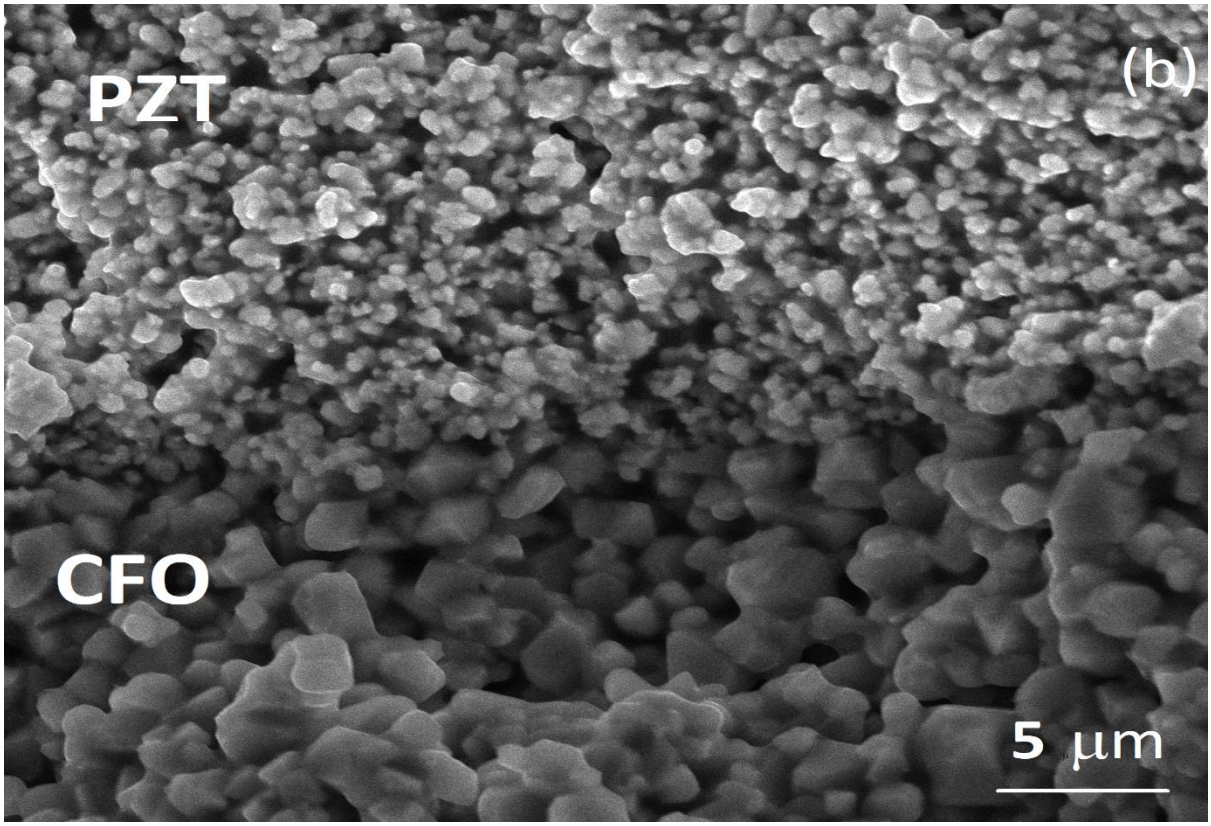

Fig. 3.b BEI SEM micrograph of the microstructure at the interface between PZT and CFO

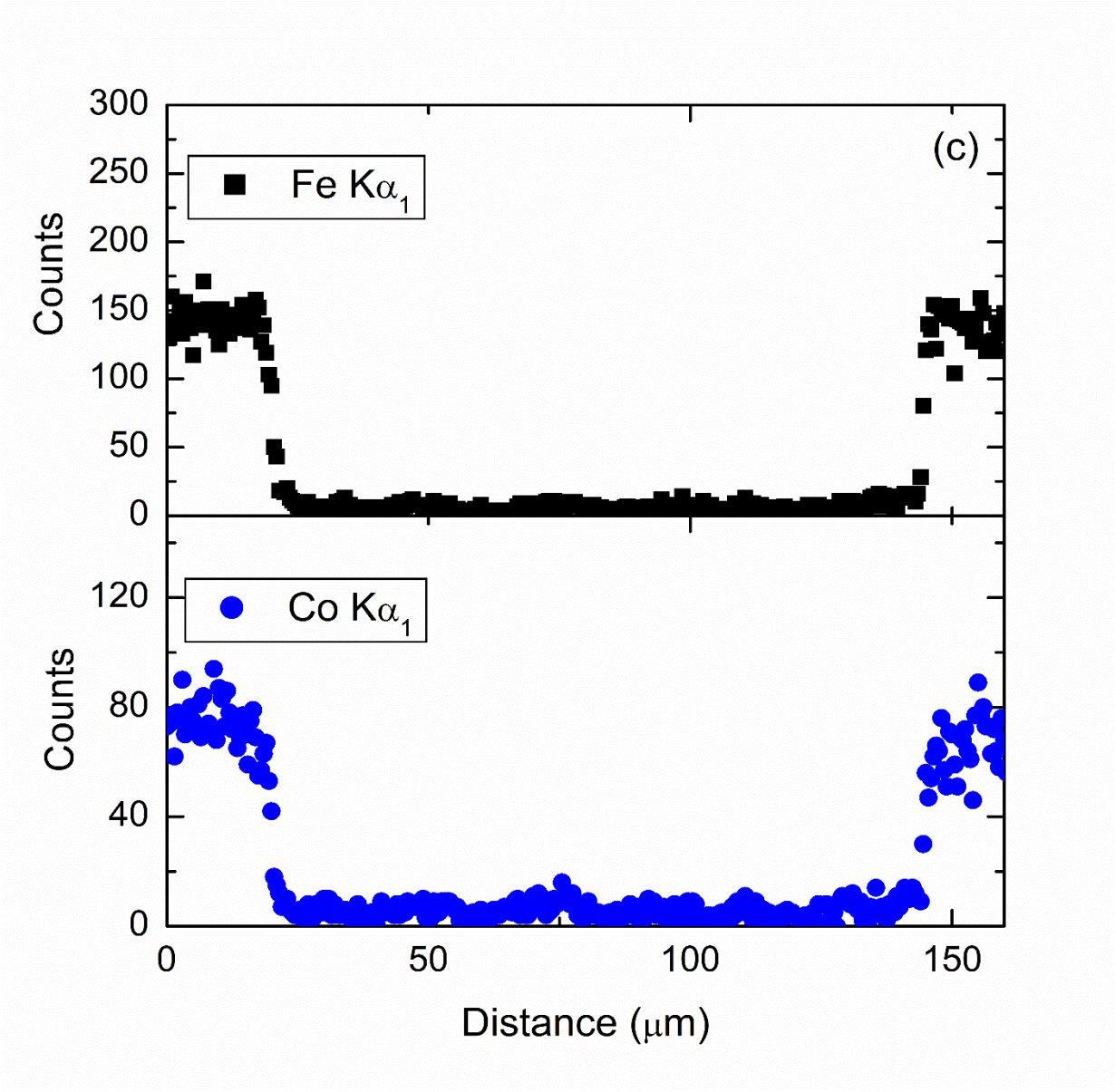

Fig. 3.c Co and Fe EDX linescans over a PZT layer encompassed between two CFO layers

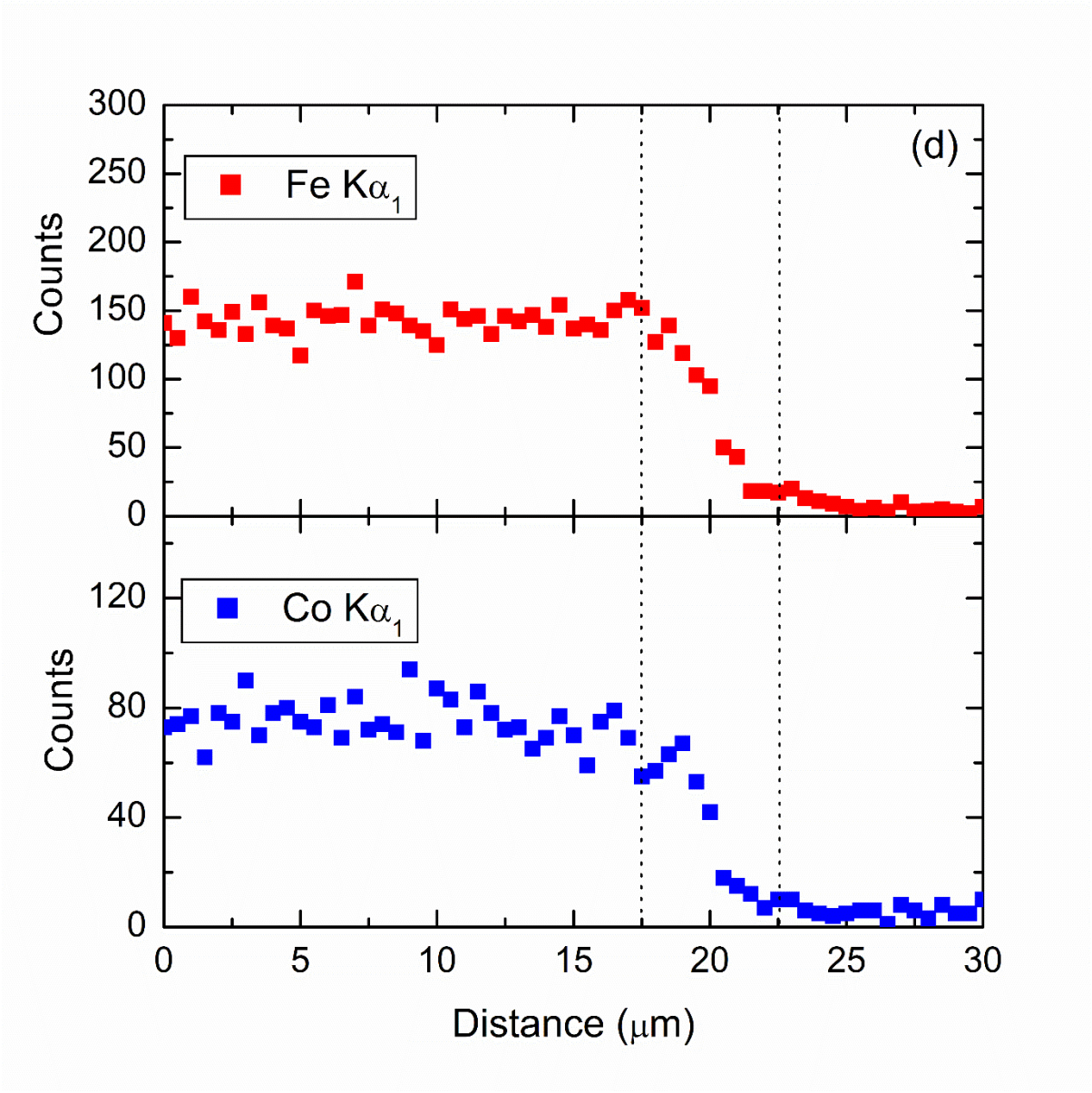

Fig. 3.d Co and Fe EDX linescans at the interface between PZT and CFO.

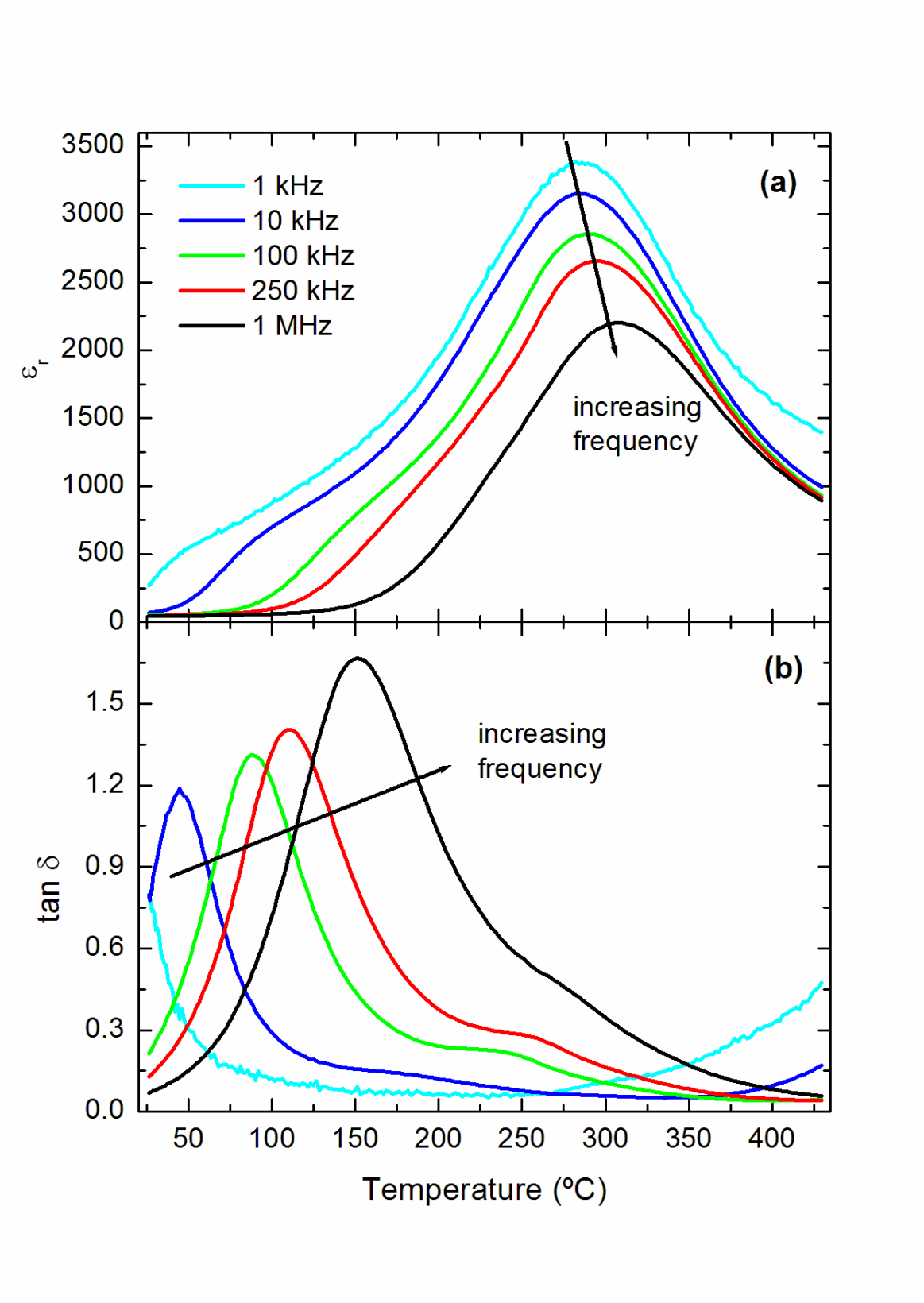

Fig. 4 Temperature dependence of the (a) relative permittivity, ε_r, and (b) dielectric loss, tan δ, for the PZT-CFO multilayers fabricated at 1050°C for 2h.

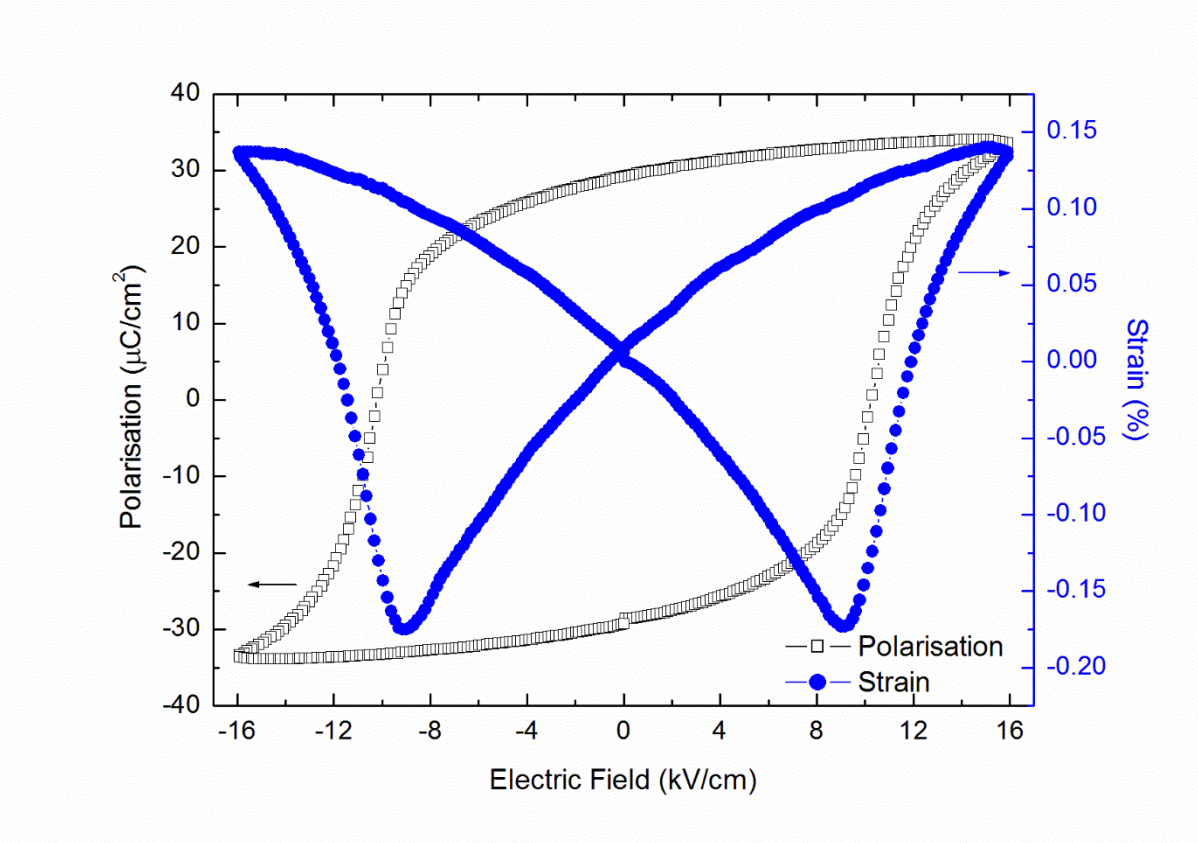

Fig. 5 Electromechanical response of a commercial PIC 151 ceramic disk with $Pb_{0.99}[(Zr_{0.45}Ti_{0.47}(Ni_{1/3}Sb_{2/3})_{0.08}]O_3$) composition.

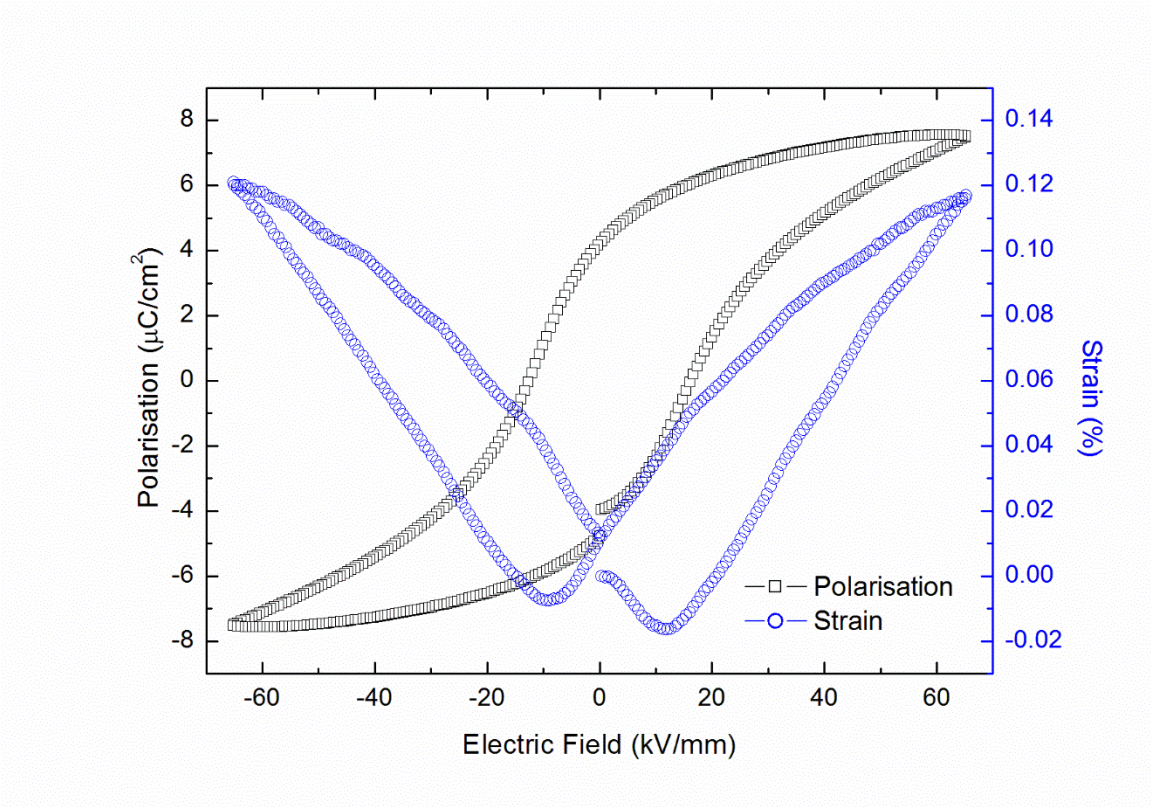

Fig. 6 Electromechanical response for the PZT-CFO multilayers fabricated at 1050°C for 2h.

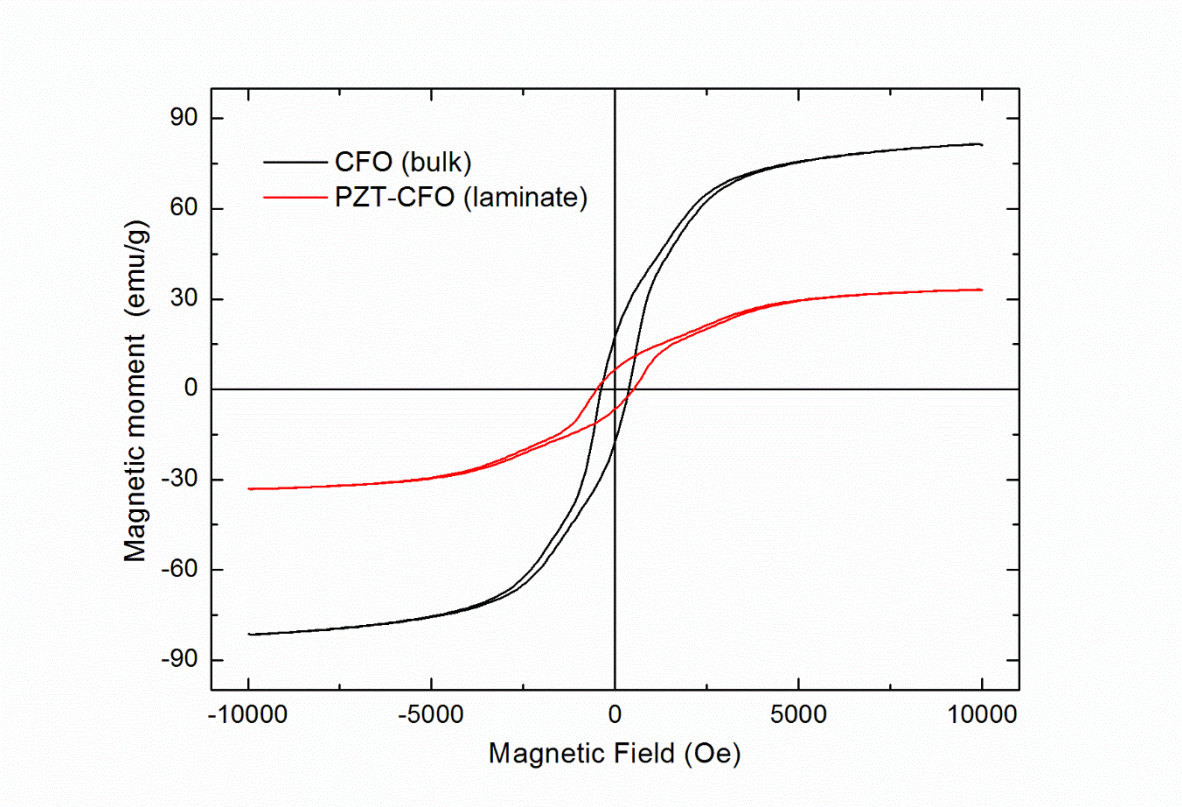

Fig. 7 Room-temperature M(H) loops for CFO and PZT-CFO multilayers fabricated at 1050°C for 2h.

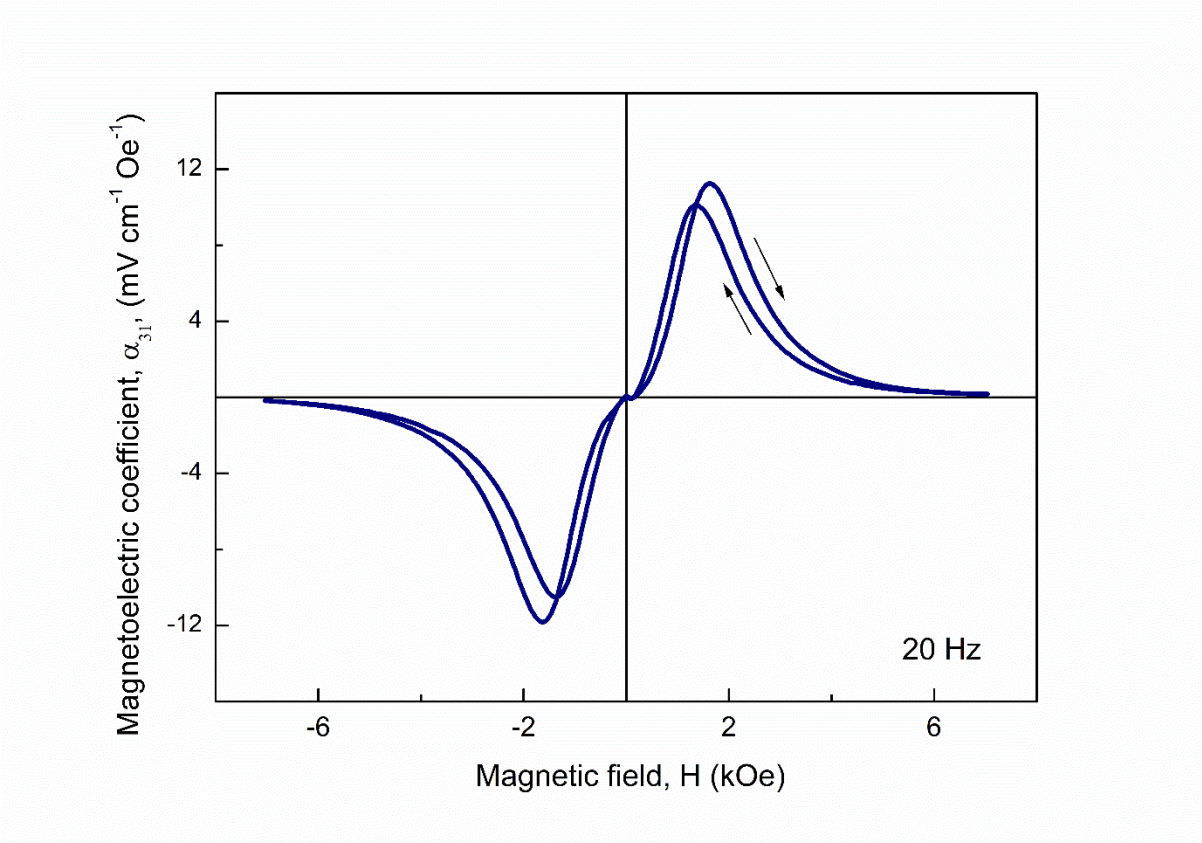

Fig. 8 ME coupling measurement for PZT-CFO multilayers fabricated at 1050°C for 2h.